Mater. Res. Soc. Symp. Proc. Vol. 1245 © 2010 Materials Research Society 1245-A07-01

Effects of Grain Boundaries on Performance of Hydrogenated Nanocrystalline Silicon Solar Cells

Tining Su[1], David Bobela[2], Xixiang Xu[1], Scott Ehlert[1], Dave Beglau[1], Guozhen Yue[1], Baojie Yan[1], Arindam Banerjee[1], Jeff Yang[1], and Subhendu Guha[1]
[1]United Solar Ovonic LLC, 1100 West Maple Road, Troy, MI, 48084, U.S.A.
[2]National Renewable Energy Laboratory, 1617 Cole Blvd, Golden, CO, 80401, U.S.A.

ABSTRACT

We investigate the effect of hydrogenation of grain boundaries on the performance of solar cells for hydrogenated nanocrystalline silicon (nc-Si:H) thin films. Using hydrogen effusion, we found that the amplitude of the lower temperature peak in the H-effusion spectra is strongly correlated to the open-circuit voltage in solar cells. This is attributed to the hydrogenation of grain boundaries in the nc-Si:H films.

INTRODUCTION

Hydrogenated nanocrystalline silicon (nc-Si:H) thin films are getting a great deal of attention for use in the bottom cell in multi-junction solar cells. The nc-Si:H based cell has excellent long wavelength response, and is less vulnerable to light-induced degradation than hydrogenated amorphous silicon (a-Si:H) based cells [1-4]. One disadvantage of the nc-Si:H solar cell is its relatively low open-circuit voltage (V_{oc}). A typical value of V_{oc} for nc-Si:H solar cells is about 0.5 V, and is often much lower. This compares poorly to about 1 V for a-Si:H cells. The lower than optimal V_{oc} for the nc-Si:H solar cells can be attributed to many reasons, such as crystalline volume fraction and the defect density in *i*-layer, as well as ambient degradation. Ambient degradation refers to degradation of V_{oc} and short-circuit current density (J_{sc}) observed for certain cells when exposed to the ambient conditions for an extended period of time. Electron-spin-resonance (ESR) in nc-Si:H films shows that the neutral defects mostly reside at the grain boundaries [5]. These defects can act as recombination centers, resulting in lower V_{oc}. In addition, it has been suggested that oxygen related defects at the grain boundaries causes increased dark current, and hence also reduced V_{oc} [6].

It has been suggested that improved hydrogenation of grain boundaries can improve V_{oc} [7]. Also, depositing the *i*-layer at lower temperatures has been shown to improve V_{oc} [6]. This was attributed to increased hydrogen concentration in the film resulting in better hydrogenation of the grain boundaries. Although it is well known that lower deposition temperature tends to reduce the crystalline volume fraction, and increase hydrogen incorporation in the films, it does not necessarily increase the degree of hydrogenation of the grain boundaries. To our best knowledge, no direct evidence has been reported that demonstrates a positive correlation between increased hydrogen concentration and increased hydrogenation of the grain boundaries. To distinguish hydrogen at the grain boundaries from that in the amorphous phase, sophisticated techniques are required for typical local probes, such as ^{1}H NMR; and interpretation of the results is not trivial. In addition, these techniques usually cannot be directly applied to solar cells, due to the presence of doped layers in the solar cells.

We use hydrogen effusion to detect different hydrogen sites in the nc-Si:H films. Hydrogen effusion has been extensively used to study hydrogenated micro-crystalline (μc-Si:H) and a-Si:H films made near the transition between amorphous and nanocrystalline phase. In μc-

Si:H made with plasma enhanced chemical vapor deposition (PECVD), the effusion peak near 400 °C is attributed to the desorption of hydrogen at the grain boundaries. These hydrogen molecules can quickly diffuse out along the paths at the grain boundaries [8,9]. In a-Si:H made with very high hydrogen dilution, an effusion peak near 400 °C was also observed [10-12]. This peak was attributed to hydrogen at the "grain boundaries" of those very small crystallites that are assumed to exist in the film, probably with a size less than 10 Å [9]. In both cases, the effusion peaks at about 400 °C are attributed to the hydrogen on the grain boundaries. Typical H-effusion spectra in nc-Si:H also exhibit this sharp peak at about 400 °C. This peak is attributed to the hydrogen sites that can find a "fast" path to the film surface, such as through the grain boundaries and columnar shaped voids, similar to the case in a-Si:H with very high hydrogen dilution and μc-Si:H. Careful comparison of this peak in solar cells made with different deposition conditions and cell performance may provide insight into the hydrogenation of the grain boundaries and the effect of such hydrogenation on cell performance.

EXPERIMENTAL

Large-area solar cells were deposited at United Solar, using modified very high frequency (MVHF). Details of MVHF technique can be found elsewhere [3]. Four small-area samples were cut from large area films deposited over a 15"x14" area for various characterizations. These cells have different V_{oc} and J_{sc} in their as-deposited states. Cell A is the reference cell, cells B and C have similar J_{sc} but different V_{oc} as sample A. Cell D shows low V_{oc} and J_{sc}, and exhibits significant ambient degradation. All four cells have similar thickness of around 2.5 μm. Table I summarizes the J-V characteristics of these four cells.

Hydrogen effusion, Raman spectroscopy, and X-Ray diffraction (XRD) spectroscopy were carried out on the whole solar cells at the National Renewable Energy Laboratory (NREL).

Table I. J-V characteristics of the samples described in the text.

Sample	V_{oc} (V)	J_{sc} (mA/cm^2)	FF (AM1.5)	FF (blue)	FF (red)	η (%)
A	0.49	24.56	0.61	0.65	0.68	7.38
B	0.42	24.09	0.50	0.57	0.58	5.03
C	0.49	24.50	0.51	0.62	0.64	6.17
D	0.41	17.05	0.52	0.61	0.60	3.62

RESULTS AND DISCUSSION

Hydrogen effusion results

Figure 1 shows the H-effusion spectra for the four cells listed in Table I. The thin black line represents the spectrum from sample A, the reference sample. The thick line, the gray dashed line, and the gray solid line represent the spectra from samples B, C, and D, respectively. For sample B, no hydrogen effusion data was obtained between 260 °C and 330 °C. The spectra are normalized to their sample volume. Therefore the amplitude of the spectra reflects the hydrogen content in these cells. In Fig. 1, samples A, B, and C all show a sharp effusion peak near 390 °C, and also increasing effusion near 600 °C. On the other hand, sample D shows only a

small increase of effused H_2 near 390 °C, and almost all the hydrogen is effused after the temperature reaches 600 °C. The hydrogen concentration in these samples is also significantly different. Samples A and C have the highest hydrogen concentration, while sample D has the lowest. In all cases, samples having a higher peak near 390 °C also have a higher peak near 600 °C.

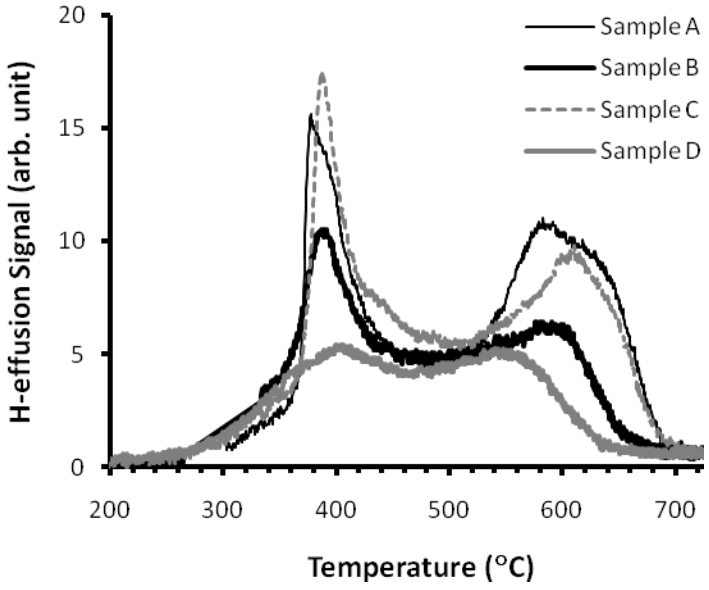

Figure 1. Hydrogen effusion spectra for the fours samples listed in Table I.

Raman results

Figure 2 shows the Raman spectra for the four samples, using 633 nm light. The black dashed line is from sample A. The gray solid line, the black solid line, and the gray dotted line are from samples B, C, and D, respectively. The crystalline volume fraction for each sample is calculated by fitting the curve with three components that are attributed to the amorphous phase, the crystalline phase, and the grain boundaries. A detailed discussion can be found elsewhere [13]. Table II lists the crystalline volume fraction in the intrinsic layer for each sample. From Table II, one can see that these four cells have very different crystalline volume fractions. The two samples with high V_{oc} and high J_{sc} both have much lower crystalline volume fractions, 25% and 36% respectively, while sample D has the highest crystalline volume fraction, 82%.

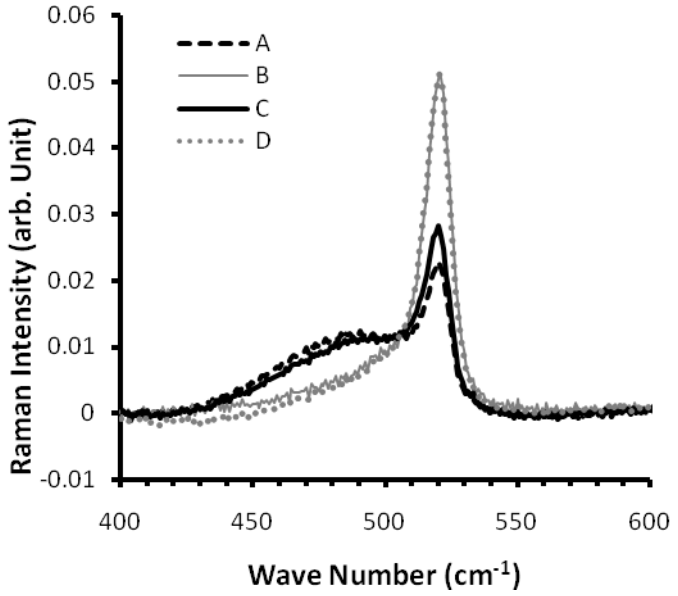

Figure 2. Raman spectra for the four samples listed in Table I.

Table II. Crystalline volume fraction obtained from Raman spectra. a-Si, GB, and c-Si indicate signals arising from the amorphous phase, the grain boundaries, and the crystalline phase, respectively. "Peak" and "σ" denote the position of the peaks and the witdth of the Gaussian functions used to fit the curves. "f_c" denotes the crystalline volume fraction in each sample.

Sample	Components	Peak (cm^{-1})	2σ (cm^{-1})	f_c
A	a-Si	485	52	0.25
	GB	514	20	
	c-Si	520	8	
B	a-Si	485	56	0.73
	GB	514	28	
	c-Si	520	8	
C	a-Si	485	50	0.36
	GB	512	26	
	c-Si	520	8	
D	a-Si	495	56	0.82
	GB	508	28	
	c-Si	520	10	

Discussion

The Raman results show that the two high performance cells, samples A and C, both have very low crystalline volume fractions. Sample A shows no ambient degradation, while sample C

shows a slight ambient degradation. On the other hand, samples B and D show severe ambient degradation after exposure to air for three months. The degree of ambient degradation were measured by the J-V characteristics and the external quantum efficiency (QE). The correlation between cell performance and crystalline volume fraction is consistent with a previous report [13]. On the other hand, the XRD results did not show any significant difference in terms of crystalline orientation in these samples; all samples have dominant orientations along (111) and (220), and similar volume fractions along each orientation.

The H-effusion results provide interesting information about the structure in the intrinsic nc-Si:H layer. A general trend is that cells with better performance have higher hydrogen content in the *i*-layer. For all four samples, the spectra intensities between 400 °C and 600 °C are rather similar, and probably represent the hydrogen in the "bulk" amorphous region. The most obvious differences are the intensities of the peak near 390 °C and 600 °C. The lower temperature peak at 390 °C is very similar for the two high performance cells (A and C). A sharp reduction of V_{oc} occurs when the intensity of this peak is reduced by about 50% (sample B), and further reduction of the peak intensity results in only a slight reduction of V_{oc} (sample D). This suggests that for sample A and C, the grain boundaries are highly hydrogenated. Since the hydrogen concentration is much higher than that of the defects, a slight reduction of hydrogenation creates enough defects on the grain boundaries to reduce V_{oc} significantly. It is also possible that when these samples are exposed to moisture and oxygen, the "exposed" sites on the grain boundaries allow for the oxygen related defects to more readily form, thus causing ambient degradation and further reducing V_{oc}.

The peak near 600 °C has been attributed to the presence of "compact" amorphous or crystalline silicon, which may form during the effusion [14], and is limited by the diffusion of atomic hydrogen in the amorphous phase. However, it is not easy to explain the occurrence of the peak unless there is a large difference in hydrogen concentration along the growth direction. It should be noted that this temperature is similar to that for the solid-state crystallization of amorphous silicon thin films. In fact, amorphous silicon films can be crystallized on a time scale of 30 minutes at 600 °C [15]. It is conceivable that crystallization can be faster in nc-Si:H films since no incubation is needed. Therefore it is possible that the peak at 600 °C is partially caused by the crystallization in these films, resulting in a rapid displacement of a large quantity of hydrogen as the crystalline volume fraction grows rapidly.

SUMMARY

In summary, we studied the correlation between the hydrogenation of grain boundaries and the V_{oc} in nc-Si:H based solar cells. Hydrogen effusion spectra suggests a strong correlation between hydrogenation of grain boundaries and V_{oc}. Higher hydrogenation of grain boundaries results in higher V_{oc}, and the dependence of V_{oc} on the hydrogenation is rather strong. This provides direct evidence of how microscopic hydrogen bonding at the grain boundaries affects the nc-Si:H cell performance.

ACKNOWLEDGEMENTS

The authors thank K. Younan, D. Wolf, T. Palmer, N. Jackett, L. Sivec, B. Hang, R. Capangpangan, J. Piner, G. St. John, A. Webster, J. Wrobel, B. Seiler, G. Pietka, C. Worrel, D. Tran, Y. Zhou, S. Liu, and E. Chen for sample preparation and measurements. We also thank H.

Fritzsche for the in-depth discussions. The work was supported by US DOE under the Solar America Initiative Program Contract No. DE-FC36-07 GO 17053.

REFERENCES

1. J. Meier, R. Flückiger, H. Keppner, and A. Shah, Appl. Phys. Lett. **65**, 860 (1994).
2. B. Yan G. Yue, and S. Guha, in *Amorphous and Polycrystalline Thin-Film Silicon Science and Technology*, edited by Virginia Chu, Seiichi Miyazaki, Arokia Nathan, Jeffrey Yang, and Hsiao-Wen Zan (Mat. Res. Soc. Symp. Proc. **989**, Pittsburgh, PA, 2007) pp. 335.
3. X. Xu, B. Yan, D. Beglau, Y. Li, G. DeMaggio, G. Yue, A. Banerjee, J. Yang, S. Guha, P. Hugger, and D. Cohen, in *Amorphous and Polycrystalline Thin-Film Silicon Science and Technology*, edited by Arokia Nathan, Andrew Flewitt, Jack Hou, Seiichi Miyazaki, and Jeffrey Yang (Mater. Res. Soc. Symp. Proc. **1066**, Pittsburgh, PA, 2008) pp. 325
4. G. Ganguly, G. Yue, B. Yan, J. Yang, S. Guha, in *Conf. Record of the 2006 IEEE 4th World Conf. on Photovoltaic Energy Conversion*, Hawaii, USA, May 7-12, 2006, p.1712.
5. T. Su, T. Ju, B. Yan, J. Yang, S. Guha, and P. C. Taylor, J. Non-Cryst. Solids, **354**, 2231 (2008)
6. Y. Nasuno, M. Kondo, and A. Matsuda, Appl. Phys. Lett. **78**, 2330 (2001).
7. M. Kondo, *et al.*, in *Proceedings of 31st IEEE PVSC* (IEEE, New York, 2005) pp. 1377 (and references therein).
8. F. Finger, K. Prasad, S. Dubail, A. Shah, X.-M Tang, J. Weber, and W. Beyer, in *Amorphous Silicon Technology*, edited by A. Madan, Y. Hamakawa, M. Thompson, P. C. Taylor, and P. G. LeComber (Mat. Res. Soc. Symp. Proc. **219**, Pittsburgh, PA, 1991) pp. 383.
9. W. Beyer, P. Harpke, and U. Zasreow, in *Amorphous and Microcrystalline Silicon Technology*, edited by E.A.Schiff, M.Hack, S.Wagner, R.Schropp, I.Shimizu (Mater. Res. Soc. Symp. Proc. **467**, Pittsburgh, PA , 1997) pp.343.
10. X. Xu, J. Yang, and S. Guha, J. Non-Cryst. Solids, **198-200**, 60 (1996).
11. S. Guha, J. Yang, A. Banerjee, B. Yan, K. Lord, Sol. Ener. Mater. Sol Cells, **78**, 329 (2003) (and references therein).
12. A. H. Mahan, J. Yang, S. Guha, and D. L. Williamson, Phys. Rev. B **61**, 1677 (2000).
13. G. Yue, B. Yan,G. Ganguly, J. Yang, S. Guha, C. W. Teplin,, and D. Williamson, in *Conf. Record of the 2006 IEEE 4th World Conf. on Photovoltaic Energy Conversion*, Hawaii, USA, May 7-12, pp. 1588 (and references therein).
14. W. Beyer, in *Tetrahedrally-Bonded Amorphous Semiconductors*, edited by S. D. Adler and H.H. Fritzshe (Plenum, New York, 1985) pp.129.
15. P. Stradins, D. Young, Y, Yan, E. Iwaniczko, Y. Xu, R. Reedy, H. Branz, and Q. Wang, Appl. Phys. Lett. **89**, 121921 (2006).